TYPE Original Research
PUBLISHED 12 February 2026
DOI 10.3389/fenrg.2024.1484676

OPEN ACCESS

EDITED BY
Shiyu Yang,
Oregon Institute of Technology, United States

REVIEWED BY
Chenhui Song,
Changsha University of Science and Technology, China
Xun Jiang,
Cardiff University, United Kingdom
Xingtang He,
Tianjin University, China

*CORRESPONDENCE
Yixuan Chen,
powergrid2024@126.com

RECEIVED 22 August 2024
ACCEPTED 29 November 2024
PUBLISHED 12 February 2026

CITATION
You G, Chen Y and Shen X (2026) Optimal configuration method for energy storage in distribution networks for enhancing power supply capability.
Front. Energy Res. 12:1484676.
doi: 10.3389/fenrg.2024.1484676

Optimal configuration method for energy storage in distribution networks for enhancing power supply capability

Guangzeng You, Yixuan Chen* and Xue Shen

Yunnan Power Grid Co., LTD., Kunming, China

To address the planning challenges of integrating energy storage into distribution networks, this paper proposes an optimal configuration method for energy storage in distribution networks aimed at enhancing power supply capability. Firstly, a total supply capability (TSC) curve model for distribution networks with integrated energy storage is introduced, which effectively represents the comprehensive power supply capability of distribution networks. Based on the TSC curve, the critical component is identified. Secondly, an optimal configuration method for energy storage with three phases is proposed to enhance the TSC curve: i) Identify the critical component; ii) Develop a preliminary configuration scheme for energy storage integration into the distribution network based on the critical component; iii) Determine the optimal energy storage configuration to improve the TSC curve. Finally, the effectiveness of the proposed method is verified by the IEEE 33-node case. The proposed method can effectively determine the optimal configuration for energy storage integration, significantly enhancing the complete power supply capability of the distribution network. This paper provides guidance on energy storage configuration in distribution networks, contributing to the efficient and low-carbon operation of the system.

KEYWORDS

distribution network, power supply capability, energy storage, optimal configuration, enhance

1 Introduction

Energy storage is a flexible component in modern distribution systems. Energy storage integration into smart distribution networks can enhance power supply and accommodation capabilities (Wang et al., 2021; Sun et al., 2024), facilitate load leveling (Calero et al., 2023; Wang et al., 2024), and optimize the operation of distribution networks (Liu et al., 2021; Tur, 2020). Therefore, investigating the optimal configuration of energy storage contributes to the efficient and low-carbon operation of distribution networks.

There has been extensive research on the optimal configuration of energy storage in distribution networks. Zhao et al. (2024) proposed an energy storage planning method based on the adaptive alternating direction method of multipliers, which improves the accommodation capability of renewable energy and reduces operational costs. Feng et al. (2024) introduced energy storage planning that considers demand response, resulting in lower operating costs and increased system flexibility. Chen et al. (2024) formulated the planning decisions for the locations and capacities of energy storage, ensuring economic operation of the system and enhancing its resilience to catastrophic weather events. Li et al. (2023) proposed an energy storage system planning method that considers multiple uncertainties, enhancing the local consumption level of renewable energy. Muqbel et al. (2022) introduced a budget-constrained planning model for distributed energy storage in unbalanced distribution networks, which effectively improves system economics. Abdeltawab and Mohamed (2022) proposed an energy storage planning method for profitability maximization, effectively reducing system upgrade costs. Zhu et al. (2023) found that appropriately configuring energy storage in high-penetration distribution networks can balance the intermittency of renewable energy power and improve system economics. Santos et al. (2022) proposed a dynamic distribution system reconfiguration technique with energy storage integration, which effectively reduces the system's energy demand and carbon emissions. Jiang et al. (2021) introduced an optimal configuration method for both stationary and mobile energy storage in distribution networks, ensuring economic operation and power supply reliability. Sun et al. (2023) presented a two-layer planning method for energy storage in response to large-scale distributed photovoltaic integration, significantly enhancing the total supply capability (TSC) and accommodation capability of the distribution network. Wu et al. (2018) analyzed the impact of energy storage integration on power supply capability and found that properly configuring energy storage within the distribution network can increase the TSC.

In summary, it is found that the proper integration of energy storage can effectively enhance the TSC of distribution networks. However, existing research on energy storage optimization primarily focuses on increasing the TSC. In reality, the complete power supply capability of a distribution network under various load and distributed generation (DG) distributions is not solely defined by TSC but rather by a TSC curve (Xiao et al., 2018; 2021; 2022), of which the TSC represents only a small portion. On the other hand, research on the TSC curve of distribution networks that include energy storage has not yet been studied, leaving the quantification of the complete power supply capability in such networks unaddressed. Additionally, no studies have explored the optimization of energy storage integration in distribution networks based on the TSC curve, which means there is currently no effective method to determine the energy storage configuration that can enhance the complete power supply capability of the system based on the TSC curve.

To effectively address the aforementioned challenges, this paper proposes a novel method for optimizing energy storage configuration in distribution networks with a focus on enhancing power supply capability. The main contributions are as follows: (1) Introduced a TSC curve model for distribution networks with integrated energy storage, which provides a quantitative assessment of the complete power supply capability in distribution networks; (2) Proposed an energy storage optimal configuration method aimed at enhancing the TSC curve, which identifies critical components and effectively determines the optimal energy storage configuration, thereby fully enhancing the power supply capability of the distribution network.

The rest of this paper is organized as follows. Section 2 introduces the TSC curve model of distribution networks with energy storage. The optimal configuration method of energy storage for enhancing the TSC curve in distribution networks is presented in Section 3. The case study is presented in Section 4. Finally, the conclusion is drawn in Section 5.

2 TSC curve of distribution networks with integrated energy storage

The TSC curve is defined as a curve composed of the total load of all secure boundary points in ascending order (Xiao et al., 2018; 2021; 2022). A secure boundary point is a secure operating point with criticality. The criticality means that any minor load increase is bound to insecurity (Xiao et al., 2018; 2021; 2022). The physical meaning of the TSC curve is the complete power supply capability range of a distribution network that satisfies security constraints. It represents the complete load supply capability of the distribution network under various load and DG distributions.

The TSC curve model with integrated energy storage is formulated in Equation 1.

$$\left\{ L_{\mathrm{TSC}} = \left\{ (i, \mathrm{Val}(\boldsymbol{W}_{\mathrm{LB},i})) \left| \begin{array}{l} \mathrm{Val}(\boldsymbol{W}_{\mathrm{LB},i}) \le \mathrm{Val}(\boldsymbol{W}_{\mathrm{LB},i+1}) \\ \mathrm{Val}(\boldsymbol{W}_{\mathrm{LB},i}) = \sum_{k=1}^{n} S_{\mathrm{LB},k} \\ i \in \{1,2,3...\} \end{array} \right. \right\} \right. \tag{1}$$

where L_{TSC} represents the TSC curve, the power supply capability $\mathrm{Val}(\boldsymbol{W}_{\mathrm{LB},i})$ of an operating point is defined as the total load, $S_{\mathrm{LB},k}$ is the apparent power of the load node k, and i is the serial number of the sampling point.

The security constraints satisfied by the TSC curve are formulated in Equations 2–5. A secure boundary point lies on the security boundary of Equation 2.

$$\left\{ \begin{array}{l} \boldsymbol{W}_{\mathrm{B},i} = \begin{bmatrix} \boldsymbol{W}_{\mathrm{LB},i} \\ \boldsymbol{W}_{\mathrm{DGB},i} \end{bmatrix} = \begin{bmatrix} [S_{\mathrm{LB},1}, S_{\mathrm{LB},2}, ..., S_{\mathrm{LB},n}]^{\mathrm{T}} \\ [S_{\mathrm{DGB},1}, S_{\mathrm{DGB},2}, ..., S_{\mathrm{DGB},h}]^{\mathrm{T}} \end{bmatrix} \in \boldsymbol{B} \\ \boldsymbol{B} = \left\{ \beta_j \middle| j = 1,2,3... \right\} \end{array} \right. \tag{2}$$

where $\boldsymbol{W}_{\mathrm{B},i}$ is the secure boundary point composed of $\boldsymbol{W}_{\mathrm{LB},i}$ and $\boldsymbol{W}_{\mathrm{DGB},i}$, $\boldsymbol{W}_{\mathrm{LB},i}$ represents the apparent power vector of the load node, $\boldsymbol{W}_{\mathrm{DGB},i}$ represents the apparent power vector of the DG node, $S_{\mathrm{DGB},h}$ denotes the apparent power of the DG node h, $\boldsymbol{B}$ represents the set of all security boundaries, and $\beta_{\mathrm{DG},j}$ is the j-th security boundary.

The secure boundary point satisfies the criticality constraint of Equation 3. This constraint means that all load variables are subject to equality constraints, which are ensured by the summation of coefficients of load variables in equality constraints being greater than zero. Equation 3 includes both reverse and forward power flow constraints. Specifically, the equality constraints indicate that the forward power flow of a component has reached its capacity, while the inequality constraints ensure that the power flow does not exceed this capacity. Equality constraints imply that once the forward power flow of a component reaches its capacity, any load cannot be further increased. In this paper, a component that reaches its forward power flow capacity under equality constraints is defined as a critical component. Identifying critical components is crucial for the optimal configuration of energy storage.

$$\beta_j = \left\{ \boldsymbol{W}_{\mathrm{B},i} \left| \begin{array}{l} (1+s)\,(b_{11}S_{\mathrm{LB},1} + \cdots + b_{1n}S_{\mathrm{LB},n} \\ +b_{1\,(n+1)}S_{\mathrm{DGB},1} + \cdots + b_{1\,(n+h)}S_{\mathrm{DGB},h} + b_{1\,(n+h+1)}S_{\mathrm{ESSB},1} + \cdots + b_{1\,(n+h+k)}S_{\mathrm{ESSB},k}) = \boldsymbol{c_1} \\ \ldots\ldots \\ (1+s)\,(b_{l1}S_{\mathrm{LB},1} + \cdots + b_{ln}S_{\mathrm{LB},n} \\ +b_{l\,(n+1)}S_{\mathrm{DGB},1} + \cdots + b_{l\,(n+h)}S_{\mathrm{DGB,h}} + b_{l\,(n+h+1)}S_{\mathrm{ESSB},1} + \cdots + b_{l\,(n+h+k)}S_{\mathrm{ESSB},k}) = \boldsymbol{c_l} \\ -c_{l+1} \leq (1+s)\left(b_{(l+1)1}S_{\mathrm{LB},1} + \cdots + b_{(l+1)\,(n+h)}S_{\mathrm{DGB},h} + \cdots + b_{(l+1)\,(n+h+k)}S_{\mathrm{ESSB},k}\right) < c_{l+1} \\ \ldots\ldots \\ -c_m \leq (1+s)\left(b_{m1}S_{\mathrm{LB},1} + \cdots + b_{m\,(n+h)}S_{\mathrm{DGB},h} + \cdots + b_{m\,(n+h+k)}S_{\mathrm{ESSB},k}\right) < c_m \\ b_{11} + b_{21} + \cdots + b_{l1} > 0, \ldots\ldots, b_{1n} + b_{2n} + \cdots + b_{ln} > 0 \end{array} \right. \right\} \tag{3}$$

where l is the number of equality constraints, m is the total number of equality and inequality constraints, b_{ln} is coefficients with values of 0 or 1, s is the network loss coefficient, and c_l is the capacity of the l-th component (branch or electrical device).

Equation 4 represents the power constraint of energy storage. The energy storage power is the minimum of the power control system (PCS)-constrained power and state of charge (SOC)-constrained power. Noted that "max" indicates the selection of the minimum absolute value from the non-positive numbers, since both quantities on the right-hand side of the $S_{\mathrm{ESS,d}}$ expression are non-positive.

$$\begin{cases} S_{\mathrm{ESSB},i} = \Upsilon S_{\mathrm{ESS,d}} + (1-\Upsilon)S_{\mathrm{ESS,c}}\ \Upsilon = 0 \text{ or } 1 \\ S_{\mathrm{ESS,d}} = \max\left(S^{\mathrm{PCS}}_{\mathrm{ESS,d}}, \dfrac{T_{\mathrm{ESS,N}}\left[Q^{\min}_{SOC} - Q_{SOC}(t)\right]}{\Delta t \lambda_{\mathrm{ESS}}}\eta_{\mathrm{ESS,d}}\right) \\ S_{\mathrm{ESS,c}} = \min\left(S^{\mathrm{PCS}}_{\mathrm{ESS,c}}, \dfrac{T_{\mathrm{ESS,N}}\left[Q^{\max}_{SOC} - Q_{SOC}(t)\right]}{\Delta t \lambda_{\mathrm{ESS}} \eta_{\mathrm{ESS,c}}}\right) \end{cases} \tag{4}$$

where $S_{\mathrm{ESSB},i}$ denotes the power of energy storage connected to node i, Υ is a binary variable, $S_{\mathrm{ESS,d}}$ is the discharging power of energy storage, $S_{\mathrm{ESS,c}}$ is the charging power of energy storage, $S^{\mathrm{PCS}}_{\mathrm{ESS,d}}$ is the maximum discharging power limits of the PCS, $S^{\mathrm{PCS}}_{\mathrm{ESS,c}}$ is the maximum charging power limits of the PCS, $T_{\mathrm{ESS,N}}$ is the energy capacity of the energy storage, $Q^{\min}_{SOC}$ is the minimum values of the SOC, $Q^{\max}_{SOC}$ is the maximum values of the SOC, Δt is the charging and discharging time of the energy storage, $\eta_{\mathrm{ESS,c}}$ is the charging efficiencies of the energy storage, $\eta_{\mathrm{ESS,d}}$ is the discharging efficiencies of the energy storage, λ_{ESS} is the power factor of the energy storage when connected to the distribution network.

Equation 5 indicates that all secure boundary points satisfy the voltage constraints.

$$\Delta \boldsymbol{U}^- \leq \Delta \boldsymbol{U}\% \leq \Delta \boldsymbol{U}^+ \tag{5}$$

where $\Delta \boldsymbol{U}$ is the voltage offset vector at nodes, $\Delta \boldsymbol{U}^-$ is the minimum voltage offset, and $\Delta \boldsymbol{U}^+$ is the maximum voltage offset. In China's low-voltage distribution network, the national standard specifies that the maximum and minimum values of $\Delta \boldsymbol{U}$ are +7% and −7%, respectively.

Note that the proposed TSC curve model is applicable in scenarios with high DG penetration. The reasons are as follows: A significant feature of distribution networks with high DG penetration is the occurrence of reverse power flow, where power flows from the feeder back to the network. In the proposed TSC curve model, both forward and reverse power flow constraints are included in Equation 3. This indicates that the model allows power flow reversal in distribution networks with abundant DG resources.

The differences between the proposed TSC curve model and existing models are as follows: The proposed TSC curve model takes into account energy storage as a flexible component, incorporating the power constraints of energy storage. It quantifies the complete power supply capability range of an active distribution network with integrated energy storage, which helps guide the optimal configuration of energy storage in the distribution network to improve system efficiency. However, the existing models (Xiao et al., 2018; 2021; 2022) do not consider energy storage and are not applicable to active distribution networks with integrated energy storage.

3 Energy storage optimal configuration for enhancing the TSC curve

The proposed optimal configuration of energy storage aimed at enhancing the TSC curve is illustrated in Figure 1 and involves three steps: 1) Identify the critical component; 2) Develop a preliminary configuration scheme for energy storage integration into the distribution network based on the critical component; 3) Determine the optimal configuration of energy storage to enhance the TSC curve.

Step 1: Identify the critical component

As defined in Section 2, critical components are those in the distribution network where the forward power flow first reaches its capacity limit, at which point any load cannot be increased. The critical components are characterized by the fact that they include all downstream load nodes and the fewest possible DG nodes. This characteristic allows for the identification of critical components in any given distribution network.

Step 2: Develop a preliminary configuration scheme for energy storage integration into the distribution network based on the critical component

Based on the critical components, the nodes in the distribution network are divided into downstream and upstream nodes relative to the critical components. Downstream nodes are those located downstream of the critical component, while upstream nodes are those located upstream. Downstream refers to the direction from the substation transformer toward the end of the feeder, and upstream refers to the direction from the feeder end back toward the substation transformer.

$\mathrm{N_S} = \{\mathrm{N}_1, \ldots, \mathrm{N}_k\}$ denotes the upstream nodes of the critical component, and $\mathrm{N_X} = \{\mathrm{N}_{k+1}, \ldots, \mathrm{N}_q\}$ denotes the downstream nodes of the critical component. N_k represents the kth node in the distribution network, and q is the total number of nodes.

To effectively enhance the power supply capability of the distribution network, the preliminary configuration scheme involves integrating energy storage at the downstream nodes of the critical components rather than at the upstream nodes.

Step 3: Determine the optimal configuration of energy storage to enhance the TSC curve

After determining the preliminary configuration scheme for energy storage, it is necessary to calculate the TSC curve and its indices for the network with integrated energy storage. Then, the impact of different configuration schemes on enhancing power supply capability is

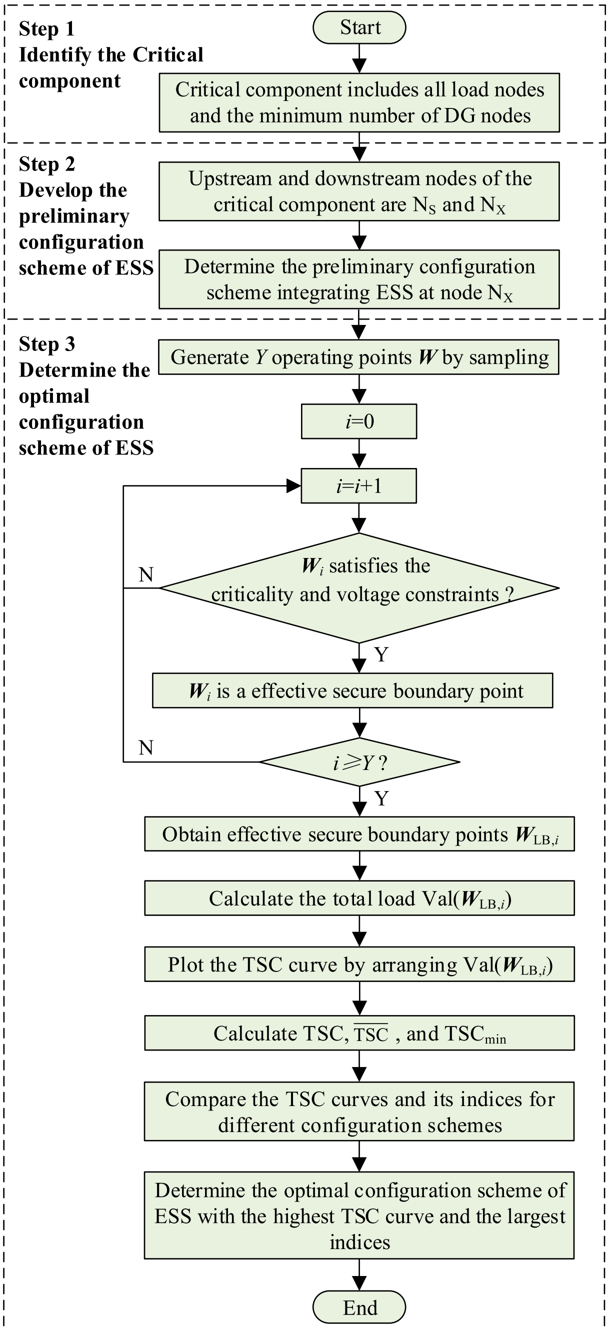

FIGURE 1
The optimal configuration flowchart of energy storage for enhancing the TSC curve.

compared. Finally, the optimal energy storage configuration that provides the most significant improvement in power supply capability is selected. The process includes the following steps:

Step 3.1: Calculate the TSC curve and its indices for distribution networks with integrated energy storage.

(1) Generate Y operating points by uniformly sampling within the capacity ranges of load nodes ($[0, S_{L,i}{}^{max}]$), energy storage nodes ($[-S_{ESS,i}{}^{max}, 0]$), and DG nodes ($[S_{DG,i}{}^{max}, 0]$) with a step size of q. The number of sampled operating points is formulated in Equation 6.

$$Y = \prod_{i=1}^{n}\left(1+\frac{S_{L,i}^{max}}{q}\right)\prod_{i=1}^{k}\left(1+\frac{S_{ESS,i}^{max}}{q}\right)\prod_{i=1}^{h}\left(1+\frac{|S_{DG,i}^{max}|}{q}\right) \tag{6}$$

where $S_{L,i}^{max}$, $S_{ESS,i}^{max}$, and $S_{DG,i}^{max}$ are the power upper limits of $S_{L,i}$, $S_{ESS,i}$, and $S_{DG,i}$, respectively.

(2) Calculate the secure boundary points

First, identify the secure boundary points from the sampled operating points that satisfy the criticality constraint of Equation 3. Then, solve the voltage offset for each secure boundary point with the power flow solver OpenDSS, thus determining the effective secure boundary points that satisfy the voltage constraints of Equation 5.

(3) Plot the TSC curve

Calculate the total load $\mathrm{Val}(\boldsymbol{W}_{LB,i})$ for effective secure boundary points using Equation 1, then plot the TSC curve by arranging $\mathrm{Val}(\boldsymbol{W}_{LB,i})$ in ascending order.

(4) Calculate the TSC curve indices

The maximum power supply capability is TSC (Xiao et al., 2018; 2021; 2022). The average power supply capability is $\overline{\mathrm{TSC}}$. The minimum power supply capability is TSC_{min}.

Step 3.2: Determine the optimal configuration scheme of energy storage by comparing the performance of different schemes in enhancing power supply capability.

Compare the TSC curves and its indices for different energy storage configuration schemes in the same figure and table. Select the configuration scheme with the highest TSC curve and the largest indices as the optimal configuration scheme of energy storage, as this configuration scheme offers the greatest comprehensive power supply capability.

4 Case study

In this section, the IEEE 33-node distribution network is used to verify the effectiveness of the proposed method. First, the TSC curve of the case is calculated, and then the optimal configuration scheme of energy storage is determined based on the TSC curve.

4.1 Case overview

As shown in Figure 2, the proposed method is verified by the IEEE 33-node distribution network. Suppose the capacity of the feeder is 1.00 MVA and each branch length is 0.25 km. The network loss coefficient s is 5%. The capacity of a planned energy storage system (ESS) is 4.00 MWh. The PCS power range of the ESS is [−1.00, 1.00]

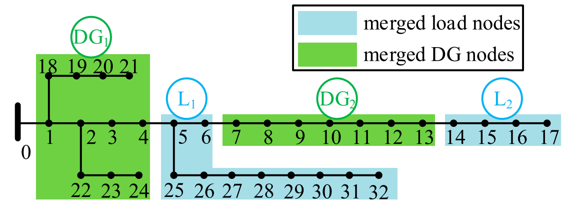

FIGURE 2
IEEE 33-node distribution network.

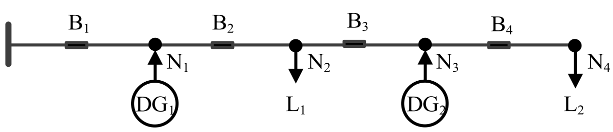

FIGURE 3
Simplified IEEE 33-node distribution network.

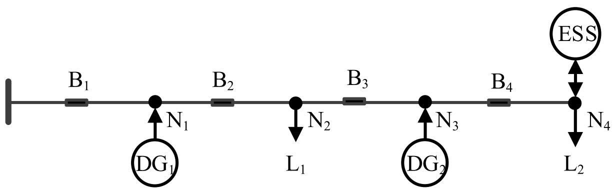

FIGURE 4
Simplified IEEE 33-node distribution network with integrated ESS.

MVA, the Q_{SOC} range is [20%, 100%], the charging and discharging time is 1 h, the grid-connected power factor is 0.90, and the charging and discharging efficiency is 0.95. Load nodes (L_1, L_2, and L_3) and DG nodes (DG_1 and DG_2) are formed by merging the adjacent nodes. The power range of the load nodes is [0, 1.50] MVA, and the power range of the DG nodes is [−1.00, 0] MVA. The simplified IEEE 33-node distribution network after equivalent merging is shown in Figure 3.

4.2 TSC curve calculation results

Using the ESS connected to node N_4 in Figure 3 as an example, the TSC curve of the simplified IEEE 33-node distribution network shown in Figure 4 is formulated in Equation 7.

$$\begin{cases} L_{TSC} = \left\{ (i, \mathrm{Val}(\boldsymbol{W}_{LB,i})) \middle| \begin{array}{l} \mathrm{Val}(\boldsymbol{W}_{LB,i}) \le \mathrm{Val}(\boldsymbol{W}_{LB,i+1}) \\ \mathrm{Val}(\boldsymbol{W}_{LB,i}) = \sum_{k=1}^{2} S_{LB,k} \\ i \in \{1,2,3...\} \end{array} \right\} \\ \boldsymbol{W}_{B,i} = \begin{bmatrix} \boldsymbol{W}_{LB,i} \\ \boldsymbol{W}_{DGB,i} \end{bmatrix} = \begin{bmatrix} [S_{LB,1}, S_{LB,2}, ..., S_{LB,n}]^T \\ [S_{DGB,1}, S_{DGB,2}, ..., S_{DGB,h}]^T \end{bmatrix} \in \boldsymbol{B} \\ \boldsymbol{B} = \{\beta_1\} \\ \beta_1 = \left\{ \boldsymbol{W}_{B,i} \middle| \begin{array}{l} (1+s)(S_{LB,1} + S_{LB,2} + S_{DGB,2} + S_{ESSB}) = 1 \\ -1 \le (1+s)(S_{LB,1} + S_{LB,2} + S_{DGB,1} + S_{DGB,2} + S_{ESSB}) < 1 \\ -1 \le (1+s)(S_{LB,2} + S_{DGB,2} + S_{ESSB}) < 1 \\ -1 \le (1+s)(S_{LB,2} + S_{ESSB}) < 1 \end{array} \right\} \\ -1 \le S_{ESSB} \le 0 \\ -7\% \le \Delta U\% \le 7\% \end{cases} \quad (7)$$

The equality constraint $(1+s)(S_{LB,1} + S_{LB,2} + S_{DGB,2} + S_{ESSB}) = 1$ in Equation 7 covers all load variables ($S_{LB,1}$ and $S_{LB,2}$), ensuring that the secure boundary points forming the TSC curve have criticality. At this point, the forward power flow reaches the feeder's capacity constraint limit of 1.00 MVA, so any minor load increase will inevitably result in an overload. For instance, if $S_{LB,1}$ increases by 0.01, the equality constraint becomes $(1+s)(S_{LB,1} + S_{LB,2} + S_{DGB,2} + S_{ESSB}) = 1.01 > 1.00$, thereby violating the capacity constraint.

4.3 Energy storage configuration scheme calculation results

According to the method discussed in Section 3, the optimal configuration scheme of ESS for the distribution network is calculated. The detailed process is as follows.

Step 1: The only critical component identified in Figure 4 is branch B_2, while the other branches (B_1, B_3, and B_4) are not critical components. The reason is that only the downstream of branch B_2 includes all load nodes (L_1 and L_2) as well as the minimum number of DG nodes (DG_2). On the other hand, the equality constraint $(1+s)(S_{LB,1} + S_{LB,2} + S_{DGB,2} + S_{ESSB}) = 1$ in Equation 7 covers all load variables ($S_{LB,1}$ and $S_{LB,2}$), corresponding to the forward power flow in branch B_2 first reaching its capacity limit, which also confirms that branch B_2 is the only critical component.

Step 2: Based on the critical component B_2, the upstream node of the critical component in the distribution network shown in Figure 4 is $N_S = \{N_1\}$, and the downstream nodes are $N_X = \{N_2, N_3, N_4\}$. Therefore, the preliminary configuration scheme is to connect the ESS to nodes $\{N_2, N_3, N_4\}$ rather than node $\{N_1\}$.

To compare and select the optimal configuration scheme of energy storage, this paper considers connecting the planned ESS to nodes N_2, N_3, and N_4, respectively.

Step 3: Calculate and compare TSC curves to determine the optimal configuration scheme of ESS. Generate 8,899,821 operating points with a step size of $q = 0.05$ MVA. For each operating point, filter out effective secure boundary points that satisfy criticality and voltage constraints based on the TSC curve expressions under different configuration schemes. The results are shown in Tables 1–4.

Based on Tables 1–4, plot the TSC curves for different configuration schemes of ESS and calculate the TSC curve indices. The results are shown in Figure 5 and Table 5.

According to Figure 5, it is concluded as follows.

(1) The complete power supply capability of the IEEE 33-node distribution network with ESS is represented by a TSC curve rather than a single value of maximum power supply capability.
(2) The TSC curves for configurations of ESS at the downstream nodes $\{N_2, N_3, N_4\}$ of critical component B_2 are overall higher

TABLE 1 The secure boundary points with the ESS connected to the downstream node N_2.

$W_{B,i}$	$S_{L,1}$/MVA	$S_{L,2}$/MVA	S_{ESS}/MVA	$S_{DG,1}$/MVA	$S_{DG,2}$/MVA	Val($W_{L,i}$)/MVA
W_1	0.20	0.75	0.00	−1.00	0.00	0.95
W_2	0.20	0.75	0.00	−0.95	0.00	0.95
W_3	0.20	0.75	0.00	−0.90	0.00	0.95
W_4	0.20	0.75	0.00	−0.85	0.00	0.95
W_5	0.20	0.75	0.00	−0.80	0.00	0.95
W_6	0.20	0.75	0.00	−0.75	0.00	0.95
...						
W_{5600}	1.25	0.45	−0.50	−0.05	−0.25	1.70
...						
W_{11195}	1.50	0.90	−0.45	−0.30	−1.00	2.40
W_{11196}	1.50	0.90	−0.45	−0.25	−1.00	2.40
W_{11197}	1.50	0.90	−0.45	−0.20	−1.00	2.40
W_{11198}	1.50	0.90	−0.45	−0.15	−1.00	2.40
W_{11199}	1.50	0.90	−0.45	−0.10	−1.00	2.40
W_{11200}	1.50	0.90	−0.45	−0.05	−1.00	2.40

TABLE 2 The secure boundary points with the ESS connected to the downstream node N_3.

$W_{B,i}$	$S_{L,1}$/MVA	$S_{L,2}$/MVA	S_{ESS}/MVA	$S_{DG,1}$/MVA	$S_{DG,2}$/MVA	Val($W_{L,i}$)/MVA
W_1	0.20	0.75	0.00	−1.00	0.00	0.95
W_2	0.20	0.75	0.00	−0.95	0.00	0.95
W_3	0.20	0.75	0.00	−0.90	0.00	0.95
W_4	0.20	0.75	0.00	−0.85	0.00	0.95
W_5	0.20	0.75	0.00	−0.80	0.00	0.95
W_6	0.20	0.75	0.00	−0.75	0.00	0.95
...						
W_{5600}	1.25	0.45	−0.50	−0.05	−0.25	1.70
...						
W_{11195}	1.50	0.90	−0.45	−0.30	−1.00	2.40
W_{11196}	1.50	0.90	−0.45	−0.25	−1.00	2.40
W_{11197}	1.50	0.90	−0.45	−0.20	−1.00	2.40
W_{11198}	1.50	0.90	−0.45	−0.15	−1.00	2.40
W_{11199}	1.50	0.90	−0.45	−0.10	−1.00	2.40
W_{11200}	1.50	0.90	−0.45	−0.05	−1.00	2.40

than those at the upstream node N_1, indicating that configuring energy storage downstream of the critical component can effectively and comprehensively enhance the power supply capability of the distribution network.

(3) Compare the configuration schemes of ESS at the downstream nodes $\{N_2,N_3,N_4\}$ of the critical component B_2 to determine the optimal configuration scheme. It can be observed that the TSC curve is highest when the ESS is configured at node N_4, indicating that configuring ESS at node N_4 provides greater power supply capability compared to nodes N_2 and N_3. Therefore, the optimal configuration scheme of ESS is to connect the ESS to the downstream node

TABLE 3 The secure boundary points with the ESS connected to the downstream node N_4.

$W_{B,i}$	$S_{L,1}$/MVA	$S_{L,2}$/MVA	S_{ESS}/MVA	$S_{DG,1}$/MVA	$S_{DG,2}$/MVA	Val($W_{L,i}$)/MVA
W_1	0.15	1.00	−0.20	−1.00	0.00	1.15
W_2	0.15	1.00	−0.20	−0.95	0.00	1.15
W_3	0.15	1.00	−0.20	−0.90	0.00	1.15
W_4	0.15	1.00	−0.20	−0.85	0.00	1.15
W_5	0.15	1.00	−0.20	−0.80	0.00	1.15
W_6	0.15	1.00	−0.20	−0.75	0.00	1.15
...						
W_{10450}	1.05	1.20	−0.75	−0.55	−0.55	2.25
...						
W_{20895}	1.50	1.30	−0.90	−0.30	−0.95	2.80
W_{20896}	1.50	1.30	−0.90	−0.25	−0.95	2.80
W_{20897}	1.50	1.30	−0.90	−0.20	−0.95	2.80
W_{20898}	1.50	1.30	−0.90	−0.15	−0.95	2.80
W_{208999}	1.50	1.30	−0.90	−0.10	−0.95	2.80
W_{20900}	1.50	1.30	−0.90	−0.05	−0.95	2.80

TABLE 4 The secure boundary points with the ESS connected to the upstream node N_1.

$W_{B,i}$	$S_{L,1}$/MVA	$S_{L,2}$/MVA	S_{ESS}/MVA	$S_{DG,1}$/MVA	$S_{DG,2}$/MVA	Val($W_{L,i}$)/MVA
W_1	0.2	0.75	−1	−0.85	0	0.95
W_2	0.2	0.75	−1	−0.8	0	0.95
W_3	0.2	0.75	−1	−0.75	0	0.95
W_4	0.2	0.75	−1	−0.7	0	0.95
W_5	0.2	0.75	−1	−0.65	0	0.95
W_6	0.2	0.75	−1	−0.6	0	0.95
...						
W_{12615}	0.95	0.8	0	−0.05	−0.8	1.75
...						
W_{25225}	1.5	0.45	0	−0.3	−1	1.95
W_{25226}	1.5	0.45	0	−0.25	−1	1.95
W_{25227}	1.5	0.45	0	−0.2	−1	1.95
W_{25228}	1.5	0.45	0	−0.15	−1	1.95
W_{25229}	1.5	0.45	0	−0.1	−1	1.95
W_{25230}	1.5	0.45	0	−0.05	−1	1.95

N_4 of the critical component B_2 in the distribution network, which most effectively enhances power supply capability.

Table 5 quantifies that the complete power supply capability of the distribution network with integrated ESS is represented as a range of values rather than a single TSC. For example, the complete power supply capability when the ESS is connected to the downstream node N_4 of the critical component B_2 in the distribution network ranges between [0.95, 2.80] MVA.

On the other hand, as shown in Table 5, although the minimum power supply capability TSC_{min} is the same, the maximum and average power supply capabilities when ESS is configured at the

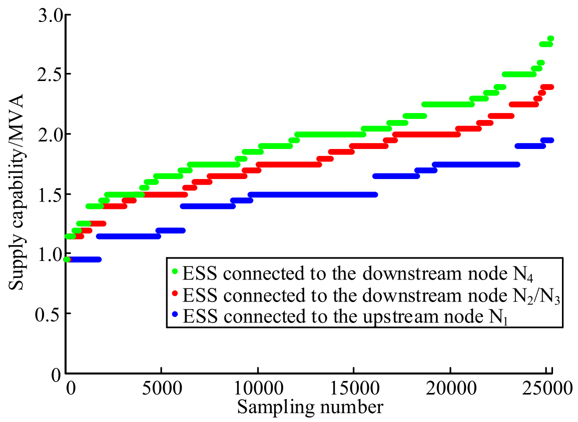

FIGURE 5
TSC curves under different configuration schemes of ESS.

downstream node N_4 are higher compared to configurations at downstream nodes $\{N_2,N_3\}$ and the upstream node N_1. It indicates that configuring ESS at the downstream node N_4 offers a greater overall power supply capability for the distribution network. Therefore, the optimal configuration scheme of ESS connected to the downstream node N_4 of the critical component B_2 in the distribution network is effective.

Noted that the selection of the sampling step size influences both the accuracy of the TSC curve and the computational time. A smaller step size enhances the curve's precision but increases the computational cost. In contrast, a larger step size improves computational efficiency at the expense of reduced accuracy. In practice applications, it is crucial to carefully choose an appropriate step size to achieve an optimal balance between accuracy and computational efficiency.

In summary, the proposed method can effectively determine the optimal configuration scheme for energy storage integration into the distribution network, maximizing both the maximum and average power supply capability of the network. Therefore, the proposed method is applicable to scenarios involving the integration of new energy storage into the distribution network.

5 Conclusion

To address the planning of energy storage in the distribution network, this paper introduces a TSC curve model for the distribution network with integrated energy storage and proposes an optimal configuration method for energy storage aimed at enhancing power supply capability. The main conclusions are summarized as follows:

(1) The proposed TSC curve model quantifies the complete power supply capability of the distribution network with integrated energy storage as a TSC curve rather than a single TSC value.
(2) The proposed method differentiates upstream and downstream nodes by identifying critical components. Compared to upstream nodes, energy storage configured at downstream nodes better enhances the overall power supply capability of the distribution network.
(3) The proposed method can determine the optimal configuration scheme for integrating energy storage into the distribution network, thereby comprehensively improving the power supply capability.

To determine effectively the configuration scheme for integrating energy storage into the distribution network is of significant value for enhancing the system's power supply capability and flexibility. The proposed method contributes to the secure, efficient, and clean low-carbon operation of the distribution network. As the computation of the TSC curve encompasses all possible load and DG distributions, it can effectively cover all the load and DG variations. The limitations of the proposed method in practical applications are as follows: The applicability of the proposed method to large-scale distribution networks is limited because the method requires a time-consuming sampling process when calculating the TSC curve. In the future, the energy storage planning of distribution networks, considering electric vehicles, the N-1 security constraints, and weather conditions on DG output power will be studied.

Data availability statement

The original contributions presented in the study are included in the article/supplementary material, further inquiries can be directed to the corresponding author.

Author contributions

GY: Conceptualization, Investigation, Methodology, Project administration, Resources, Software, Supervision, Validation, Writing–original draft. YC: Data curation, Formal Analysis, Investigation, Project administration, Software, Validation,

TABLE 5 TSC curve indices under different configuration schemes of ESS.

Configuration schemes of ESS	TSC/MVA	$\overline{TSC}$/MVA	TSC_{min}/MVA
Connected to the downstream node N_2/N_3 of critical component B_2	2.40	1.78	0.95
Connected to the downstream node N_4 of critical component B_2	2.80	1.94	0.95
Connected to the upstream node N1 of critical component B_2	1.95	1.48	0.95

Visualization, Writing–review and editing. XS: Formal Analysis, Investigation, Validation, Writing–review and editing.

Funding

The author(s) declare that financial support was received for the research, authorship, and/or publication of this article. This work was supported by the Innovation Program of China Southern Power Grid Co., Ltd., Collaborative Optimization and Control Technology of New Distribution System with High Proportion of Distributed Wind Power and Distributed Photovoltaic' Topic 2: Multi-time Scale Active Collaborative Optimization and Control Technology for New Distribution Systems for Distributed New Energy Consumption and Low-Carbon Operation (YNKJXM20222378).

Conflict of interest

Authors GY, YC, and XS were employed by Yunnan Power Grid Co., LTD.

Publisher's note

References

Abdeltawab, H., and Mohamed, Y. (2022). Energy storage planning for profitability maximization by power trading and ancillary services participation. *IEEE Syst. J.* 16 (2), 1909–1920. doi:10.1109/JSYST.2021.3069671

Calero, F., Cañizares, C., Bhattacharya, K., Anierobi, C., Calero, I., de Souza, M., et al. (2023). A review of modeling and applications of energy storage systems in power grids. *P. IEEE* 111 (7), 806–831. doi:10.1109/JPROC.2022.3158607

Chen, H., Xiong, X., Zhu, J., Wang, J., Wang, W., and He, Y. (2024). A two-stage stochastic programming model for resilience enhancement of active distribution networks with mobile energy storage systems. *IEEE T. Power Deliv.* 39 (4), 2001–2014. doi:10.1109/TPWRD.2023.3321062

Feng, P., Chen, C., and Wang, L. (2024). Coordinated energy storage and network expansion planning considering the trustworthiness of demand-side response. *Front. Energy Res.* 12, 1384760. doi:10.3389/fenrg.2024.1384760

Jiang, X., Chen, J., Zhang, W., Wu, Q., Zhang, Y., and Liu, J. (2021). Two-step optimal allocation of stationary and mobile energy storage systems in resilient distribution networks. *J. Mod. Power Syst. Cle.* 9 (4), 788–799. doi:10.35833/MPCE.2020.000910

Li, J., Xu, Z., Liu, H., Wang, C., Wang, L., and Gu, C. (2023). A wasserstein distributionally robust planning model for renewable sources and energy storage systems under multiple uncertainties. *IEEE T. Sustain. Energ.* 14 (3), 1346–1356. doi:10.1109/TSTE.2022.3173078

Liu, H., Zhao, Y., Gu, C., Ge, S., and Yang, Z. (2021). Adjustable capability of the distributed energy system: definition, framework, and evaluation model. *Energy* 222, 119674. doi:10.1016/j.energy.2020.119674

Muqbel, A., Al-Awami, A., and Parvania, M. (2022). Optimal planning of distributed battery energy storage systems in unbalanced distribution networks. *IEEE Syst. J.* 16 (1), 1194–1205. doi:10.1109/JSYST.2021.3099439

Santos, S., Gough, M., Fitiwi, D., Pogeira, J., Shafie-khah, M., and Catalão, J. (2022). Dynamic distribution system reconfiguration considering distributed renewable energy sources and energy storage systems. *IEEE Syst. J.* 16 (3), 3723–3733. doi:10.1109/JSYST.2021.3135716

Sun, B., Jing, R., Ge, L., Zeng, Y., Dong, S., and Hou, L. (2024). Quick hosting capacity evaluation based on distributed dispatching for smart distribution network planning with distributed generation. *J. Mod. Power Syst. Cle.* 12 (1), 128–140. doi:10.35833/mpce.2022.000604

Sun, X., Huang, B., Yan, H., Li, P., Zu, Y., and Li, X. (2023). Energy storage planning method for improving power supply capacity and renewable energy consumption in county distribution station. *2023 Power Electron. Power Syst. Conf. (PEPSC)*, 323–327. doi:10.1109/PEPSC58749.2023.10395605

Tur, M. (2020). Reliability assessment of distribution power system when considering energy storage configuration technique. *IEEE Access* 8, 77962–77971. doi:10.1109/ACCESS.2020.2990345

Wang, B., Zhang, C., Dong, Z., and Li, X. (2021). Improving hosting capacity of unbalanced distribution networks via robust allocation of battery energy storage systems. *IEEE T. Power Syst.* 36 (3), 2174–2185. doi:10.1109/TPWRS.2020.3029532

Wang, G., Wang, C., Feng, T., Wang, K., Yao, W., and Zhang, Z. (2024). Day-ahead and intraday joint optimal dispatch in active distribution network considering centralized and distributed energy storage coordination. *IEEE T. Ind. Appl.* 60 (3), 4832–4842. doi:10.1109/TIA.2024.3372943

Wu, W., Zhou, J., Yu, H., and Guo, Z. (2018). Power supply capability evaluation of power grid containing integrated charging-discharging-storage station. *Power Syst. Technol.* 42 (4), 1266–1273. doi:10.13335/j.1000-3673.pst.2017.0202

Xiao, J., Cai, Z., Liang, Z., and She, B. (2022). Mathematical model and mechanism of TSC curve for distribution networks. *Electr. Power Energy Syst.* 137, 107812. doi:10.1016/j.ijepes.2021.107812

Xiao, J., Wang, C., She, B., Li, F., Bao, Z., and Zhang, X. (2021). Total supply and accommodation capability curves for active distribution networks: concept and model. *Electr. Power Energy Syst.* 133, 107279. doi:10.1016/j.ijepes.2021.107279

Xiao, J., Zhang, M., Bai, L., She, B., and Zhang, B. (2018). Boundary supply capability for distribution systems: concept, indices and calculation. *IET Gener. Transm. Dis.* 12 (2), 499–506. doi:10.1049/iet-gtd.2017.0725

Zhao, L., Zhang, J., Wang, Y., Zhang, Z., Gao, P., and Zhang, R. (2024). AADMM based shared energy storage planning for resilience improvement of renewable energy stations. *Front. Energy Res.* 12, 1467627. doi:10.3389/fenrg.2024.1467627

Zhu, H., Li, H., Liu, G., Ge, Y., Shi, J., Li, H., et al. (2023). Energy storage in high variable renewable energy penetration power systems: technologies and applications. *CSEE J. Power Energy* 9 (6), 2099–2108. doi:10.17775/CSEEJPES.2020.00090

Nomenclature

L_{TSC}	TSC curve
$\mathrm{Val}(W_{\mathrm{LB},i})$	Power supply capability of the operating point
$W_{\mathrm{B},i}$	Secure boundary point
$W_{\mathrm{LB},i}$	Apparent power vector of the load node
$W_{\mathrm{DGB},i}$	Apparent power vector of the DG node
$S_{\mathrm{LB},k}$	Apparent power of the load node k
$S_{\mathrm{DGB},h}$	Apparent power of the DG node h
B	All security boundaries
β_j	j-th security boundary
c_l	The l-th component capacity
l	Number of equality constraints
m	Total number of equality and inequality constraints
s	Network loss coefficient
$S_{\mathrm{ESSB},k}$	Energy storage power connected to node k
$S_{\mathrm{ESS},d}$	Energy storage discharging power
$S_{\mathrm{ESS},c}$	Energy storage charging power
$S_{\mathrm{ESS,d}}^{\mathrm{PCS}}$	Maximum discharging power of the PCS
$S_{\mathrm{ESS,c}}^{\mathrm{PCS}}$	Maximum charging power of the PCS
$T_{\mathrm{ESS,N}}$	Energy storage energy capacity
$Q_{SOC}^{\max}$	Maximum values of the SOC
$Q_{SOC}^{\min}$	Minimum values of the SOC
Δt	Charging and discharging time
$\eta_{\mathrm{ESS,c}}$	Charging efficiencies of the energy storage
$\eta_{\mathrm{ESS,d}}$	Discharging efficiencies of the energy storage
λ_{ESS}	Energy storage power factor
ΔU	Voltage offset vector
ΔU^{+}	Maximum voltage offset
ΔU^{-}	Minimum voltage offset.